Resistivity of Non-Galilean-Invariant Two-Dimensional Dirac Systems

V. M. Kovalev,[1,2] M. V. Entin,[1,3] Z. D. Kvon,[1,3] A. D. Levin,[4] V. A. Chitta,[4] G. M. Gusev,[4] and N. N. Mikhailov[1,3]
[1]*Institute of Semiconductor Physics, Novosibirsk 630090, Russia*
[2]*Novosibirsk State Technical University, Novosibirsk 630073, Russia*
[3]*Novosibirsk State University, Novosibirsk 630090, Russia*
[4]*Instituto de Física da Universidade de São Paulo, 135960-170, São Paulo, São Paulo, Brazil*

(Received 15 October 2024; accepted 28 April 2025; published 15 May 2025)

We revisited the influence of electron-electron scattering on the resistivity of a two-dimensional system with a linear spectrum. In conventional systems with a parabolic spectrum, where umklapp scattering is either prohibited or ineffective due to the small Fermi surface, particle-particle scattering does not contribute to conductivity because it does not change the total momentum. However, within the framework of the Boltzmann kinetic model, we demonstrate that electron-electron scattering in Dirac systems can significantly contribute to conductivity, producing distinct temperature-dependent corrections: a T^4 behavior at low temperatures and a T^2 dependence at moderate temperatures. While the predicted T^4 scaling is not observed experimentally—likely suppressed by dominant weak localization effects—the T^2 scaling is clearly confirmed in our measurements. Specifically, temperature-dependent resistivity data from a gapless single-valley HgTe quantum well exhibit T^2 corrections, which align well with theoretical predictions. Thus, we challenge the paradigm that the T^2 term in resistivity is absent in single-band 2D metals.

DOI: 10.1103/PhysRevLett.134.196303

Introduction—The transport properties of strongly interacting systems pose a significant challenge in modern physics. One long-standing issue is the century-old debate regarding how electron-electron scattering contributes to resistivity, which is often theorized to follow a $\rho \sim T^2$ behavior [1]. Despite this expectation, experimentally detecting this T^2 behavior and attributing it directly to electron-electron interactions has proven difficult and remains largely inconclusive [2,3].

This quadratic temperature resistivity contribution only emerges when the Fermi surface is open and crosses the boundary of the Brillouin zone. Under these conditions, electrons can transfer momentum to the lattice by jumping between opposite sections of the Fermi surface. However, the resulting resistance is not a universal property; it is highly sensitive to the details of the Fermi surface topology. Furthermore, a collision integral representing electron-electron interactions that do not transfer momentum to the lattice fails to impact resistivity, unless the electric current is independent of the momentum density [4].

Consequently, the influence of electron-electron interactions on transport properties can be identified through several mechanisms for non-Galilean-invariant systems: (a) the presence of specific Fermi surface characteristics that enable umklapp scattering [4], (b) in compensated semimetals [5,6], (c) in two-subband systems with different effective masses and impurity scattering time [7–11], and (d) through electronic hydrodynamic effects in narrow channels [12–21].

It is important to note that perturbation theory predicts that unlike the Galilean-invariant case where not only the T^2 term but all higher-order terms are absent, the finite-T terms may appear for a nonparabolic spectrum. A qualitative theoretical analysis in [4] states that it should be a T^4 behavior. However, this situation has not yet been studied in detail. Here, we prove both theoretically (using the same approach as in paper [4]) and experimentally that the resistivity of a degenerate electron system with linear-in-momentum spectrum behaves as T^2.

Materials with a Dirac-like spectrum, such as graphene, require more detailed theoretical and experimental study due to several specific features in their spectrum and transport properties. First, compensated graphene is a pure material and should exhibit resistance dominated by electron-electron interactions. It is essential to recognize that at the charge neutrality point, thermal excitation of both electrons and holes facilitates the investigation of electron-electron limited transport in the nongenerated regime [22]. Furthermore, graphene samples are fabricated using exfoliation techniques, resulting in mesoscopic dimensions. In such cases, the channel size affects electron-electron limited transport (Gurzhi effect), while a thorough transport analysis generally necessitates macroscopic samples. Additionally, much of the research has concentrated on bilayer graphene, where the energy spectrum approaches parabolic characteristics at low energies [23–25].

Recognizing the importance of new quantum materials with a linear spectrum, it is essential to search for materials that can serve as effective platforms for studying interaction-affected transport. Gapless HgTe quantum wells present such an opportunity due to their high mobility and the ability to control carrier density. In this Letter, we theoretically investigate the contribution of electron-electron scattering in systems with a linear spectrum far from the Dirac point. We derive a T^2 term in the conductivity, a conclusion that is quite general and applicable to any system exhibiting a linear spectrum. Experimentally, we tested this prediction in a specific gapless HgTe quantum well and found reasonable agreement with our theoretical results. Thus, our findings confirm that the T^2 term in resistivity is indeed present in single-band 2D Dirac metals.

Theory—The theoretical model we consider is as follows: We assume that there is a two-dimensional single-band material with a linear dispersion characterized by the constant band parameter v having the velocity dimension. Thus, in the framework of this model, the energy dispersion of degenerate charge carriers with momentum $\mathbf{p}$ is given by the expression $\varepsilon_{\mathbf{p}} = vp$. We assume the charge carriers to be electrons. Such a theoretical model is directly related to the experimental structure considered in the next section.

At zero temperature, the system resistance is determined by the electron scattering off impurities characterized by the constant scattering time τ_i. At finite temperatures, the temperature-dependent correction to the resistance is due to interparticle scattering processes. At finite but low enough temperatures, when the electron-electron scattering processes are characterized by the scattering time τ_{ee}, the temperature-dependent correction to the resistivity can be found via a successive approximation with respect to small parameter $\tau_{ee} \gg \tau_i$, considering the interelectron scattering integral in the Boltzmann transport equation perturbatively.

The Bolzmann equation describing the electron interaction with external electric field $\mathbf{E}$, random impurity potential, and with other electrons reads $-(\mathbf{F}\cdot\nabla_{\mathbf{p}})f_{\mathbf{p}} = -(f_{\mathbf{p}} - n_{\mathbf{p}})/\tau_i + Q_{ee}\{f_{\mathbf{p}}\}$. Here, $\mathbf{F} = e\mathbf{E}$, where $e > 0$ is an absolute value of electron charge, $n_{\mathbf{p}}$ is an equilibrium electron distribution function, and Q_{ee} is an electron-electron collision integral. We apply here the simple τ_i approximation for the electron-impurity collision integral.

In the limit $\tau_{ee} \gg \tau_i$, the interparticle collision integral can be considered as a correction. Expanding the nonequilibrium distribution function into the first order with respect to the external force $\mathbf{F}$ as $f_{\mathbf{p}(\mathbf{k})} = n_{\mathbf{p}} + \delta f_{\mathbf{p}}$, the linear-in-$\mathbf{F}$ correction is decomposed into the electron-impurity scattering contribution, and the contribution related to electron-electron scattering $\delta f_{\mathbf{p}} = \delta f^{(0)}_{\mathbf{p}} + \delta f^{(1)}_{\mathbf{p}}$. Here, $\delta f^{(0)}_{\mathbf{p}}$ and $\delta f^{(1)}_{\mathbf{p}}$ are the iteration corrections with respect to the small term Q_{ee}. Deploying the method of successive iterations results in $\delta f^{(0)}_{\mathbf{p}} = \tau_i(\mathbf{F}\cdot\mathbf{v}_{\mathbf{p}})n'_{\mathbf{p}}$ and $\delta f^{(1)}_{\mathbf{p}} = \tau_i Q_{ee}\{\delta f^{(0)}_{\mathbf{p}}\}$.

The electron-electron-collision-induced electric current density correction reads as $\mathbf{j} = -e\tau_i\sum_{\mathbf{p}}\mathbf{v}_{\mathbf{p}}Q_{ee}\{\delta f^{(0)}_{\mathbf{p}}\}$. After cumbersome calculations [26], we arrive at the expression describing the current density correction induced by the interparticle collisions in the form

$$\begin{aligned}\mathbf{j} = {} & 2\pi e\tau_i^2\sum_{\mathbf{p},\mathbf{k},\mathbf{q}}|U_{\mathbf{q}}|^2(n_{\mathbf{p}} - n_{\mathbf{p}-\mathbf{q}})(n_{\mathbf{k}} - n_{\mathbf{k}+\mathbf{q}}) \\ & \times(\mathbf{F}\cdot\mathbf{v}_{\mathbf{p}})[\mathbf{v}_{\mathbf{p}} + \mathbf{v}_{\mathbf{k}} - \mathbf{v}_{\mathbf{p}-\mathbf{q}} - \mathbf{v}_{\mathbf{k}+\mathbf{q}}] \\ & \times\int_{-\infty}^{+\infty}\frac{d\omega}{4T\sinh^2(\frac{\omega}{2T})}\delta(\epsilon_{\mathbf{k}+\mathbf{q}} - \epsilon_{\mathbf{k}} - \omega)\delta(\epsilon_{\mathbf{p}-\mathbf{q}} - \epsilon_{\mathbf{p}} + \omega).\end{aligned} \tag{1}$$

Here, $U_{\mathbf{q}}$ is a Fourier transform of interparticle interacting potential. This is a general expression for the current correction. It is easy to see that for Galilean-invariant systems, $\mathbf{v}_{\mathbf{p}} = \mathbf{p}/m$, and the total velocity under collision in Eq. (1) vanishes $\mathbf{v}_{\mathbf{p}} + \mathbf{v}_{\mathbf{k}} - \mathbf{v}_{\mathbf{p}-\mathbf{q}} - \mathbf{v}_{\mathbf{k}+\mathbf{q}} = (\mathbf{p} + \mathbf{k} - \mathbf{p} + \mathbf{q} - \mathbf{k} - \mathbf{q})/m = 0$. This is not the case for the Galilean-noninvariant system, say, for systems with linear dispersion $\varepsilon_{\mathbf{p}} = vp$. Indeed, the corresponding velocity reads $\mathbf{v}_{\mathbf{p}} = v\mathbf{p}/p = v^2\mathbf{p}/\epsilon_{\mathbf{p}}$, where $p = |\mathbf{p}|$ is an absolute value of the particle momentum. Thus, the velocity factor $\mathbf{v}_{\mathbf{p}} + \mathbf{v}_{\mathbf{k}} - \mathbf{v}_{\mathbf{p}-\mathbf{q}} - \mathbf{v}_{\mathbf{k}+\mathbf{q}} = v^2(\mathbf{p}\epsilon_{\mathbf{p}}^{-1} + \mathbf{k}\epsilon_{\mathbf{k}}^{-1} - (\mathbf{p}-\mathbf{q})\epsilon_{\mathbf{p}-\mathbf{q}}^{-1} - (\mathbf{k}+\mathbf{q})\epsilon_{\mathbf{k}+\mathbf{q}}^{-1})$ does not vanish under the momentum conservation condition, resulting in the nonzero contribution to the current Eq. (1). The conductivity correction induced by interparticle scattering is directly related to the current density Eq. (1) in the non-Galilean-invariant system. The lengthy analysis [26] yields ($\varepsilon_q = vq$),

$$\sigma_{xx} = -\tfrac{1}{\pi^3}\left(\tfrac{e\tau_i}{4v}\right)^2\left(\tfrac{1}{T}\right)\int_{-\infty}^{+\infty}\tfrac{\omega^4 d\omega}{\sinh^2(\omega/2T)}\int_{|\omega|/v}^{\infty}\tfrac{qdq}{2\pi}\tfrac{|U_{\mathbf{q}}|^2}{\varepsilon_q^2}. \tag{2}$$

The final integration requires the particular form of an interparticle interaction potential $U_{\mathbf{q}} = 2\pi e^2/\varepsilon(q + q_s)$, where q_s is wave vector related to the screening effects due to the presence of mobile carriers. Below, we present the comparison of this expression with experimental data. It should be noted that the expression Eq. (2) was formally found via a perturbation procedure over the small parameter $\tau_i/\tau_{ee} \ll 1$ and may formally hold up to $\tau_i/\tau_{ee} \leq 1$. In the region $\tau_i/\tau_{ee} \geq 1$, our approach is not applicable, and a more sophisticated self-consistent method must be used [28,29]. Taking into account the bare Drude conductivity for particles with linear Dirac spectrum $\sigma_0 = (e^2/4\hbar)(\mu\tau_i/\hbar)$, where μ is the Fermi level of degenerate electrons, the correction to resistivity reads

$$\frac{\delta\rho}{\rho_0} = \frac{8}{\pi^2}\left(\frac{e^2}{\epsilon\hbar v}\right)^2\left(\frac{T}{\mu}\right)\left(\frac{T\tau}{\hbar}\right)\mathfrak{F}_T, \tag{3}$$

$$\mathfrak{F}_T = \left(\frac{T}{T^*}\right)^2 \int_0^\infty \frac{x^4 dx}{\sinh^2(x)} \left[\ln\left(1+\frac{T^*}{xT}\right) - \frac{1}{1+xT/T^*}\right], \tag{4}$$

where $T^\star = \hbar v q_s = (\mu e^2/\varepsilon\hbar v)$ is the characteristic temperature separating different temperature regimes [26]. The parameter $q_s = 2\mu e^2/\epsilon v^2$ represents the screening wave vector for mobile carriers with a linear spectrum. One can expect that at low temperatures ($T \ll T^\star$), $\mathfrak{F}_T \to (T/T^\star)^2 \ln T$, and the corrections are given by $\sigma_{xx} \sim T^4 \ln(2\mu/T)$. At high temperatures ($T \gg T^\star$), $\mathfrak{F}_T \to$ const, and the corrections follow $\sigma_{xx} \sim T^2$.

Experiment—HgTe-based quantum wells have attracted considerable attention due to their ability to generate a range of unconventional quantum materials, which are influenced by the quantum well's thickness. Notably, the energy spectrum of a gapless HgTe quantum well with a width of 6.3–6.5 nm features a single-valley Dirac cone at the center of the Brillouin zone. This characteristic makes the system quite similar to graphene. However, due to the single-valley structure, the electronic properties differ significantly from those of the multivalley graphene. In this HgTe well, Dirac fermions exhibit a linear energy spectrum for both electrons and holes given by $\varepsilon_p = \pm v|p|$, where the Fermi velocity is $v = 7 \times 10^7$ cm/s $= c/430$ (with c being the speed of light) and k representing the momentum [30].

The inset of Fig. 1 illustrates the variation in resistivity as a function of the gate voltage for samples A and B at a temperature of 5 K. The resistance displays a pronounced peak at the charge neutrality point corresponding to the zero-energy level. This behavior is characteristic of gapless semiconductors, such as graphene. The maximum electron density observed corresponds to a Fermi energy of approximately 150 meV.

We fabricated quantum wells using $HgTe/Cd_xHg_{1-x}Te$ material with a [013] surface orientation. The wells had equal widths, with d_0 measuring 6.7 nm. The devices used in this Letter were multiterminal bars with three consecutive segments, each 50 μm wide, and varying lengths of 100, 250, and 100 μm [26]. A 200 nm SiO_2 dielectric layer was deposited on the sample surface, which was then covered by a TiAu gate. The density variation with gate voltage was estimated to be approximately 0.9×10^{11} cm^{-2}/V calculated from the dielectric thickness and Hall measurements. Figures 1(a) and 1(b) display the variation of resistance with the gate voltage across a broad temperature range, specifically for the gate voltage interval corresponding to the electronic part of the spectrum. The plot shows a notable increase in resistance as the temperature rises, with one exception: In the temperature range 5 K $< T <$ 20 K, a reduction in resistance with increasing temperature is observed. This phenomenon can be attributed to the weak localization effect, which has been previously reported in the studies [26,27].

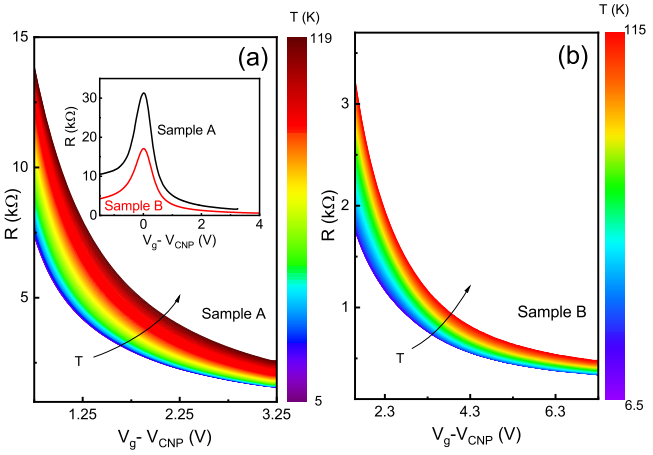

FIG. 1. Resistance as a function of the gate voltage at different temperatures for samples A (a) and sample B (b) for the electron side of the energy spectrum. Inset: resistance as a function of the gate voltage at for two gapless HgTe quantum wells, $T = 5$ K.

To further explore the temperature-dependent behavior of resistance (or resistivity), we calculate the ratio of the excess resistivity to resistivity at $T = 5$ K denoted as $\Delta\rho(T)/\rho(T = 5\text{ K}) = [\rho(T) - \rho(T = 5\text{ K})]/\rho(T = 5\text{ K})$. Figure 2 presents the excess resistance for different electron densities across a wide temperature range for both samples A and B. The main feature of the experimental dependences shown in Fig. 2 is the presence of two distinct regimes with fundamentally different temperature behaviors, separated by an excess resistance minimum at $T^* \sim (10 - 20)$ K. The value of T^* varies slightly between different samples and electron densities.

In the low-temperature regime ($T < T^*$), the excess resistance increases slightly as the temperature approaches

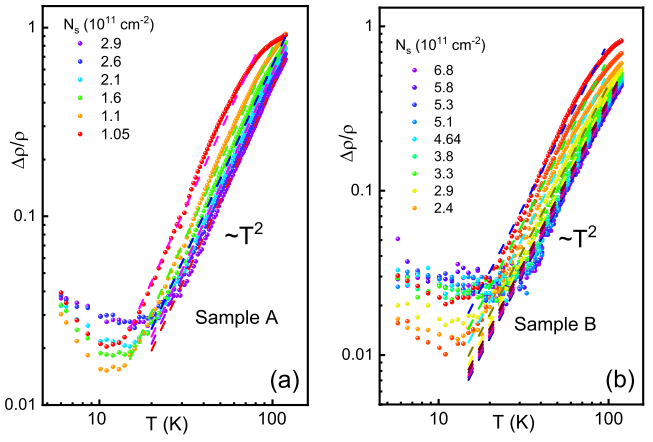

FIG. 2. Excess resistivity $\Delta\rho(T) = [\rho(T) - \rho(T = 5\text{ K})]/\rho(T = 5\text{ K})$ as a function of the temperature for various densities for samples A (a) and B (b). The dashes show the T^2 dependence calculated from Eq. (6).

zero; we attribute this behavior to weak localization effects. Conversely, in the high-temperature regime ($T > T^*$), the excess resistivity follows a T^2 dependence across all measured electron densities. This behavior suggests a dominant contribution from electron-electron scattering to the excess resistance. It is important to note that phonon scattering results in a linear temperature dependence [31]. An evaluation of the scattering time indicates that it is significantly smaller than what we observed in our temperature range. If this were not the case, we would expect to see strong deviations of $\rho(T)$ from the T^2 dependence, which is not observed (see Fig. 2).

A comparison involves matching the experimental behavior with the theoretical expression in Eq. (3). Notably, Eq. (3) also exhibits two distinct temperature regimes with different scaling behaviors. As we mentioned above, we find that at low temperatures ($T \ll T^*$), Eq. (3) gives a correction $\sigma_{xx} \sim T^4 \ln(2\mu/T)$. As $T \to 0$, this contribution becomes negligible, leaving only the dominant weak localization behavior observed experimentally In contrast, at higher temperatures $T \gg T^*$, Eq. (3) yields

$$\sigma_{xx} = -\frac{e^2}{6\hbar}\left(\frac{e^2}{\varepsilon\hbar v}\right)^2\left(\frac{T\tau_i}{\hbar}\right)^2, \tag{5}$$

$$\frac{\delta\rho}{\rho_0} = -\frac{\sigma_{xx}}{\sigma_0} = \frac{2}{3}\left(\frac{\hbar}{\tau_{ee}}\right)\left(\frac{\tau_i}{\hbar}\right), \tag{6}$$

where $(\hbar/\tau_{ee}) = (Ce^2/\varepsilon\hbar v)^2(T^2/\mu) = (C\alpha_{ee})^2(T^2/\mu)$ is an inverse electron-electron scattering time, and $\alpha_{ee} = 3.2/\epsilon$, where C is a parameter considered below. Equation (6) is the interparticle collision correction to the system resistivity for the case of degenerate electrons with a linear Dirac spectrum. Note, however, that the simplified form of the Coulomb potential does not account for either the finite thickness of the quantum well or dynamic screening effects within the random phase approximation. The relaxation of various perturbation types in a 2D Fermi gas was theoretically analyzed in Ref. [32]. Calculations of both weak- and strong-interaction limits demonstrated that the scattering time τ_{ee} depends critically on the interaction parameter $r_s = 1/(\sqrt{\pi n}a_B)$, where a_B is the Bohr radius. To achieve better agreement with theoretical predictions, we introduce an additional fitting parameter C in our analysis.

We compare Eq. (6) with the experimental curves shown in Fig. 2 by adjusting the parameters τ_i and the Coulomb interaction constant C in the expression (6). We take $\epsilon = 10$. Figure 2 shows the theoretical curves for the parameters listed in Table I. It can be observed that the experimental data closely follow the expected trend $\Delta\rho(T)/\rho(T = 5\ \mathrm{K}) \sim T^2$. For a system of massless Dirac fermions, the parameter C is given by [33] $C \approx 4\{\ln[\mu/kT]\}^{1/2}$, which approximately aligns with our extracted parameter for high-density conditions. It is important to highlight that, despite the electron-electron scattering time being closely related to hydrodynamic flow in an electron liquid, this approach predicts a temperature dependence of resistivity $\rho \sim T^{-2}$ [12,17,26], which is inconsistent with our experimental results.

TABLE I. Fitting parameters in Eq. (6) for samples A and B.

Sample	$\tau_i(10^{-12}$ s)	μ (meV)	C
A	0.56	62	2.6
A	0.47	51	3
A	0.41	45	3.2
B	1.7	92.8	1.5
B	1.4	70.8	1.6
B	1	56.8	2

A theoretical estimate of the characteristic temperature T^* using material parameters from the experimental samples yields $T^* \sim (150\text{–}170)$ K. This value exceeds the experimentally observed range of $T^* \sim (10\text{–}20)$ K by an order of magnitude. We attribute this discrepancy to limitations in our theoretical model, which assumes perfect two dimensionality and neglects finite sample width effects. These approximations lead to an incomplete treatment of screening phenomena, ultimately resulting in an overestimated T^* value. It is worth noting that additional effects, such as the renormalization of the Fermi velocity due to electron-electron (e-e) interactions, may also play a role, as theoretically predicted in various models (for a review, see Ref. [34]). Crucially, however, this renormalization is expected to be most pronounced near the Dirac point. The experimentally observed logarithmic velocity renormalization [35] is in agreement with theoretical predictions, offering direct evidence that long-range e-e interactions can significantly alter the Dirac cone structure in the vicinity of the Dirac point. However, our Letter focuses on energy regimes far from the Dirac point, where we believe such renormalization effects are not significant and are unlikely to influence transport properties. Although we did not observe a T^4 dependence in our HgTe quantum well, we expect graphene monolayers to better approximate the model interaction due to their screened Coulomb potential, with a characteristic temperature $T^* \approx 100$ K. Consequently, the T^4 contribution should be more readily observable at low temperatures in graphene. Despite the significant interest in Dirac materials, temperature-dependence studies have primarily focused on the Dirac point regime, where electron-hole plasma effects dominate [36]. A more systematic investigation of the temperature scaling across different carrier densities could help clarify the nature of the Coulomb potential in these systems.

In conclusion, we have theoretically and experimentally studied the T-dependent corrections to the resistivity due to electron-electron interactions in systems with a p-linear spectrum. These effects are absent in Galilean-invariant

systems with a parabolic spectrum. We believe that electronic transport phenomena are far from fully understood, and our research demonstrates that electron-electron-dominated transport is significantly influenced by material properties, including the shape of the Fermi surface and the dispersion relation. Among the Dirac materials, graphene, including its moiré and twisted forms, remains a fascinating and promising subject for investigating the contribution of *e-e* scattering to resistivity [37]. Transition metal dichalcogenide (TMD) systems have also gained significant attention recently in the study of *e-e* interaction effects. However, the linear spectrum approach in TMDs requires extremely high electron densities, which poses experimental challenges [38]. A particularly promising Dirac cone system has been observed in thin films of Cd_3As_2 [39]. Three-dimensional topological insulators host Dirac cone states on their surfaces, making them a fascinating platform for investigating the interplay between electron-electron interactions and topological effects. Understanding this relationship could provide deeper insights into their transport properties [40].

Acknowledgments—We acknowledge the financial support for this work provided by Sao Paulo Research Foundation Grant No. 2019/16736-2 and No. 2021/12470-8, the National Council for Scientific and Technological Development, Ministry of Science and Higher Education of the Russian Federation, and Foundation for the Advancement of Theoretical Physics and Mathematics "BASIS." The HgTe quantum wells growth and preliminary transport measurements are supported by Russian Science Foundation (Grant No. 23-72-30003).

[1] W. J. de Haas, J. de Boer, and G. J. van dën Berg, The electrical resistance of gold, copper and lead at low temperatures, Physica (Amsterdam) **1**, 609 (1934).
[2] F. J. Pinski, P. B. Allen, and W. H. Butler, Calculated electrical and thermal resistivities of Nb and Pd, Phys. Rev. B **23**, 5080 (1981).
[3] Kamran Behnia, On the origin and the amplitude of T-square resistivity in Fermi liquids, Ann. Phys. (Berlin) **534**, 2100588 (2022).
[4] H. K. Pal, V. I. Yudson, and D. L. Maslov, Reistivity of non Galilean invariant term Fermi and non Fermi liquids, Lith. J. Phys. **52**, 142 (2012).
[5] E. B. Olshanetsky, Z. D. Kvon, M. V. Entin, L. I. Magarill, N. N. Mikhailov, and S. A. Dvoretsky, Scattering processes in a two-dimensional semimetal, JETP Lett. **89**, 290 (2009).
[6] M. V. Entin, L. I. Magarill, E. B. Olshanetsky, Z. D. Kvon, N. N. Mikhailov, and S. A. Dvoretsky, The effect of electron-hole scattering on transport properties of a 2D semimetal in the HgTe quantum well, J. Exp. Theor. Phys. **117**, 933 (2013).
[7] E. H. Hwang and S. Das Sarma, Temperature dependent resistivity of spin-split subbands in GaAs two-dimensional hole systems, Phys. Rev. B **67**, 115316 (2003).
[8] K. E. Nagaev and A. A. Manoshin, Electron-electron scattering and transport properties of spin-orbit coupled electron gas, Phys. Rev. B **102**, 155411 (2020).
[9] K. E. Nagaev, Electron-electron scattering and conductivity of disordered systems with a Galilean-invariant spectrum, Phys. Rev. B **106**, 085411 (2022).
[10] G. M. Gusev, A. D. Levin, E. B. Olshanetsky, Z. D. Kvon, V. M. Kovalev, M. V. Entin, and N. N. Mikhailov, Interaction-dominated transport in two-dimensional conductors: From degenerate to partially degenerate regime, Phys. Rev. B **109**, 035302 (2024).
[11] A. D. Levin, G. M. Gusev, F. G. G. Hernandez, E. B. Olshanetsky, V. M. Kovalev, M. V. Entin, and N. N. Mikhailov, Interaction-controlled transport in a two-dimensional massless-massive Dirac system: Transition from degenerate to nondegenerate regimes, Phys. Rev. Res. **6**, 023121 (2024).
[12] R. N. Gurzhi, Minimum of resistance in impurity-free conductors, Sov. Phys. JETP **44**, 771 (1963); Sov. Phys. Usp. **11**, 255 (1968).
[13] Marco Polini and Andre K. Geim, Viscous electron fluids, Phys. Today **73**, No. 6, 28 (2020).
[14] Boris N. Narozhny, Hydrodynamic approach to two-dimensional electron systems, Riv. Nuovo Cimento Soc. Ital. Fis. **45**, 661 (2022).
[15] M. J. M. de Jong and L. W. Molenkamp, Hydrodynamic electron flow in high-mobility wires, Phys. Rev. B **51**, 13389 (1995).
[16] R. Krishna Kumar, D. A. Bandurin, F. M. D. Pellegrino, Y. Cao, A. Principi, H. Guo, G. H. Auton, M. Ben Shalom, L. A. Ponomarenko, G. Falkovich, K. Watanabe, T. Taniguchi, I. V. Grigorieva, L. S. Levitov, M. Polini, and A. K. Geim, Superballistic flow of viscous electron fluid through graphene constrictions, Nat. Phys. **13**, 1182 (2017).
[17] A. V. Andreev, Steven A. Kivelson, and B. Spivak, Hydrodynamic description of transport in strongly correlated electron systems, Phys. Rev. Lett. **106**, 256804 (2011).
[18] G. M. Gusev, A. D. Levin, E. V. Levinson, and A. K. Bakarov, Viscous electron flow in mesoscopic two-dimensional electron gas, AIP Adv. **8**, 025318 (2018).
[19] G. M. Gusev, A. D. Levin, E. V. Levinson, and A. K. Bakarov, Viscous transport and Hall viscosity in a two-dimensional electron system, Phys. Rev. B **98**, 161303(R) (2018).
[20] G. M. Gusev, A. S. Jaroshevich, A. D. Levin, Z. D. Kvon, and A. K. Bakarov, Stokes flow around an obstacle in viscous two-dimensional electron liquid, Sci. Rep. **10**, 7860 (2020).
[21] G. M. Gusev, A. S. Jaroshevich, A. D. Levin, Z. D. Kvon, and A. K. Bakarov, Viscous magnetotransport and Gurzhi effect in bilayer electron system, Phys. Rev. B **103**, 075303 (2021).
[22] K. I. Bolotin, K. J. Sikes, J. Hone, H. L. Stormer, and P. Kim, Temperature-dependent transport in suspended graphene, Phys. Rev. Lett. **101**, 096802 (2008).
[23] G. Wagner, D. X. Nguyen, and S. H. Simon, Transport in bilayer graphene near charge neutrality: Which scattering

mechanisms are important?, Phys. Rev. Lett. **124**, 026601 (2020).
[24] Y. Nam, D.-K. Ki, D. Soler-Delgado, and A. F. Morpurgo, Electron-hole collision limited transport in charge-neutral bilayer graphene, Nat. Phys. **13**, 1207 (2017).
[25] Cheng Tan, Derek Y. H. Ho, Lei Wang, Jia I. A. Li, Indra Yudhistira, Daniel A. Rhodes, Takashi Taniguchi, Kenji Watanabe, Kenneth Shepard, Paul L. McEuen, Cory R. Dean, Shaffique Adam, and James Hone, Dissipation-enabled hydrodynamic conductivity in a tunable bandgap semiconductor, Sci. Adv. **8**, 8481 (2022).
[26] wSee Supplemental Material at http://link.aps.org/supplemental/10.1103/PhysRevLett.134.196303 for a detailed solution of the Boltzmann equation related to electron-impurity and electron-electron scattering, as well as descriptions of the samples and measurement details. Supplemental Material also contains Refs. [12,17,27].
[27] D. A. Kozlov, Z. D. Kvon, N. N. Mikhailov, and S. A. Dvoretskii, Weak localization of Dirac fermions in HgTe quantum wells, JETP Lett. **96**, 730 (2012).
[28] Woo-Ram Lee, Alexander M. Finkel'stein, Karen Michaeli, and Georg Schwiete, Role of electron-electron collisions for charge and heat transport at intermediate temperatures, Phys. Rev. Res. **2**, 013148 (2020).
[29] Woo-Ram Lee, Alexander M. Finkel'stein, and Georg Schwiete, Role of electron-electron collisions for magneto-transport at intermediate temperatures, Phys. Rev. B **102**, 245117 (2020).
[30] B. Büttner, C. X. Liu, G. Tkachov, E. G. Novik, C. Brüne, H. Buhmann, E. M. Hankiewicz, P. Recher, B. Trauzettel, S. C. Zhang, and L. W. Molenkamp, Single valley Dirac fermions in zero-gap HgTe quantum wells, Nat. Phys. **7**, 418 (2011).
[31] Ye. O. Melezhik, J. V. Gumenjuk-Sichevska, and F. F. Sizov, Electron relaxation and mobility in the inverted band quantum well CdTe/$Hg_{1-x}Cd_xTe$/CdTe, Semi. Phys. Quant. Electron. Optoelectron. **17**, 85 (2014).
[32] P. S. Alekseev and A. P. Dmitriev, Viscosity of two-dimensional electrons, Phys. Rev. B **102**, 241409(R) (2020).
[33] B. N. Narozhny and M. Schutt, Magnetohydrodynamics in graphene: Shear and Hall viscosities, Phys. Rev. B **100**, 035125 (2019).
[34] Valeri N. Kotov, Bruno Uchoa, Vitor M. Pereira, F. Guinea, and A. H. Castro Neto, Electron-electron interactions in graphene: Current status and perspectives, Rev. Mod. Phys. **84**, 1067 (2012).
[35] D. C. Elias, R. V. Gorbachev, A. S. Mayorov, S. V. Morozov, A. A. Zhukov, P. Blake, L. A. Ponomarenko, I. V. Grigorieva, K. S. Novoselov, F. Guinea, and A. K. Geim, Dirac cones reshaped by interaction effects in suspended graphene, Nat. Phys. **7**, 701 (2011).
[36] Na Xin, James Lourembam, Piranavan Kumaravadivel, A. E. Kazantsev, Zefei Wu, Ciaran Mullan, Julien Barrier, Alexandra A. Geim, I. V. Grigorieva, A. Mishchenko, A. Principi, V. I. Fal'ko1, L. A. Ponomarenko, A. K. Geim1, and Alexey I. Berdyugin, Giant magnetoresistance of Dirac plasma in high-mobility graphene, Nature (London) **616**, 270 (2023)..
[37] Alexandre Jaoui, Ipsita Das, Giorgio Di Battista, Jaime Díez-Mérida, Xiaobo Lu, Kenji Watanabe, Takashi Taniguchi, Hiroaki Ishizuka, Leonid Levitov, and Dmitri K. Efetov, Quantum critical behaviour in magic-angle twisted bilayer graphene, Nat. Phys. **18**, 633 (2022).
[38] Sajedeh Manzeli, Dmitry Ovchinnikov, Diego Pasquier, Oleg V. Yazyev, and Andras Kis, 2D transition metal dichalcogenides, Nat. Rev. Mater. **2**, 17033 (2017).
[39] Luca Galletti, Timo Schumann, Omor F. Shoron, Manik Goyal, David A. Kealhofer, Honggyu Kim, and Susanne Stemmer, Two-dimensional Dirac fermions in thin films of Cd_3As_2, Phys. Rev. B **97**, 115132 (2018).
[40] M. Z. Hasan and C. L. Kane, Colloquium: Topological insulators, Rev. Mod. Phys. **82**, 3045 (2010).